DEVELOPMENTAL DYNAMICS 226:654–662, 2003

ARTICLE

Apparent Mitochondrial Asymmetry in *Xenopus* Eggs

Natalia Volodina, James M. Denegre, and Kimberly L. Mowry*

Cell polarity is manifest along the animal/vegetal axis in eggs of the frog, *Xenopus laevis*. Along this axis, maternal cytoplasmic components are asymmetrically distributed and are thought to underlie specification of distinct cell fates. To ascertain the molecular identities of such cytoplasmic components, we have used a monoclonal antibody that specifically stains the vegetal hemisphere of *Xenopus* eggs. The antigenic protein Vp67 (vegetal protein of 67 kDa) was identified through purification and cloning as a *Xenopus* homolog of the mitochondrial protein dihydrolipoamide acetyltransferase, a component of the pyruvate dehydrogenase complex. The identification of Vp67 as a mitochondrial protein could indicate that populations of mitochondria are asymmetrically distributed in *Xenopus* eggs. *Developmental Dynamics 226:654–662, 2003.* © 2003 Wiley-Liss, Inc.

Key words: *Xenopus*; oocyte; egg; subtractive immunization; mitochondria; dihydrolipoamide acetyltransferase; pyruvate dehydrogenase complex

Received 2 October 2002; Accepted 11 December 2002

INTRODUCTION

Restricted spatial distribution of cytoplasmic components within oocytes and eggs can be the basis for the development of morphological polarity in embryos. For example, the vegetal cortex of *Xenopus* oocytes and eggs harbors maternal determinants implicated in germ layer specification, dorsoventral axis specification, and germline determination (reviewed in Chan and Etkin, 2001). After fertilization, such cytoplasmic determinants are differentially distributed among the cleavage cells, resulting in specification of cell fates and establishment of the embryonic axes (reviewed in Chan and Etkin, 2001). Thus, the identities of asymmetrically distributed maternal components has been of significant interest.

In *Xenopus* eggs and oocytes, polarity along the animal/vegetal (AV) axis is evident by the asymmetric distribution of cytoplasmic components, including proteins, mRNAs, and organelles (reviewed in Danilchik and Gerhart, 1987; Gard, 1995; Chang et al., 1999; Mowry and Cote, 1999; Wylie, 1999). One of the first manifestations of polarity in the developing *Xenopus* oocyte is the presence of a mitochondrial cloud within the vegetal hemisphere of immature (stage I; Dumont, 1972) oocytes (Heasman et al., 1984). Subsequently, dynamic reorganization of the cytoskeleton (Gard, 1999) and localization of specific mRNAs and protein (reviewed in Mowry and Cote, 1999) occur during defined periods during growth of the oocyte, resulting in molecular asymmetry along the AV axis of the fully grown oocyte. By the end of oogenesis, polarity is also externally evident, with pigment restricted to the animal hemisphere and yolk platelets being larger and more abundant in the vegetal hemisphere (Danilchik and Gerhart, 1987). Importantly, the AV axis represents an axis of developmental polarity, such that embryonic cell fates along this axis are distinct (reviewed in Chan and Etkin, 2001).

To identify and characterize proteins that may be asymmetrically distributed along the AV axis of *Xenopus* eggs, we previously generated monoclonal antibodies against epitopes enriched in the vegetal hemisphere of *Xenopus* eggs by the

Department of Molecular Biology, Cell Biology and Biochemistry, Brown University Providence, Rhode Island
Grant sponsor: National Science Foundation; Grant number: IBN-9728053.
Dr. Volodina's present address is CereMedix, Inc., 120 Forsyth Street, Boston, MA 02115.
Dr. Denegre's present address is The Mount Desert Island Biological Laboratory, Salisbury Cove, ME 04672.
*Correspondence to: Kimberly L. Mowry, Department of Molecular Biology, Cell Biology and Biochemistry, Brown University, Box G-J2, Providence, RI 02912. E-mail: kimberly_mowry@brown.edu

DOI 10.1002/dvdy.10275

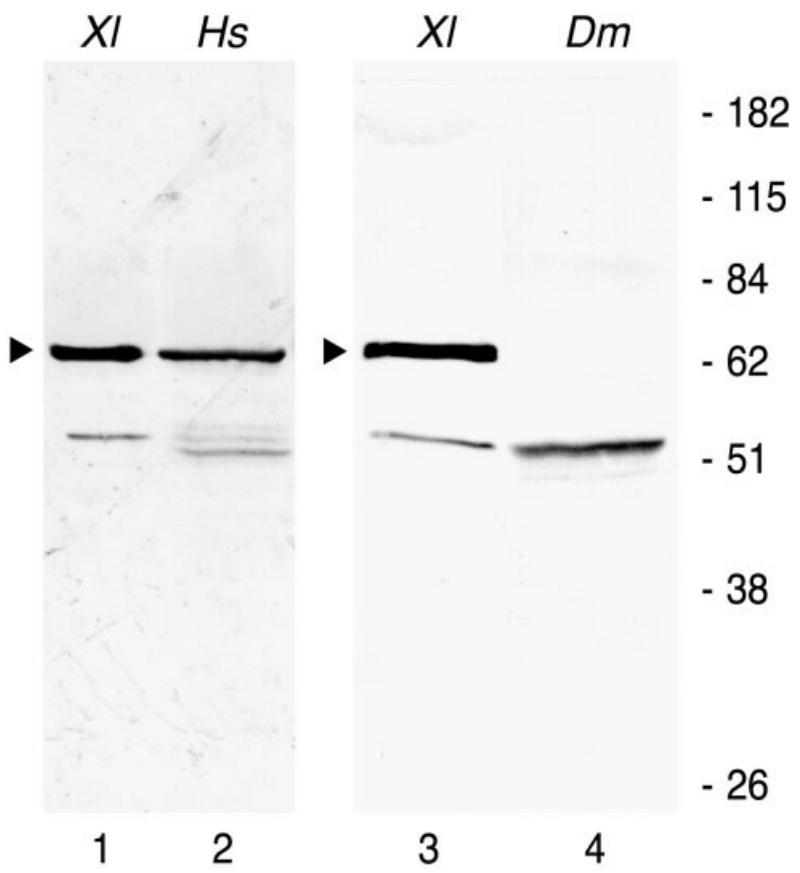

Fig. 1. Western blot analysis of Vp67 in *Xenopus* (Xl), *Drosophila* (Dm), and human (Hs) cells. Total protein homogenates of *Xenopus* eggs (lane 1), human HL-60 cells (lane 2), *Xenopus* oocytes (lane 3), and *Drosophila* early embryos (lane 4) were separated by 10% sodium dodecyl sulfate-polyacrylamide gel electrophoresis and blotted with anti-Vp67 antibody. Molecular mass markers (in kDa) are noted at the right. The position of *Xenopus* Vp67 protein is indicated by arrowheads.

proteomics technique of subtractive immunization (Denegre et al., 1997). These antibodies demonstrated a strong polarity in the cortex of the fertilized egg; immunofluorescent confocal microscopy revealed staining confined to the vegetal cortical and subcortical region, with no staining observed in the animal hemisphere cortex (Denegre et al., 1997). In the current study, one of these antibodies was used to purify the recognized antigenic protein, Vp67 (vegetal protein of 67 kDa). Purification and cloning reveals Vp67 to be a *Xenopus* homolog of the mitochondrial protein dihydrolipoamide acetyltransferase, the E2 component of the pyruvate dehydrogenase complex (PDC-E2).

RESULTS

Asymmetric distribution of protein antigens along the AV axis of *Xenopus* eggs was observed using antibodies developed by Denegre et al. (1997). In that study, indirect immunofluorescence analysis showed the protein antigens to be restricted to the vegetal hemisphere of the egg (Denegre et al., 1997). Here, we have focused on one of these antibodies (D5-5G7), which recognizes a protein antigen of approximately 67 kDa from *Xenopus* oocytes and eggs, as determined by Western blot analysis (Denegre et al., 1997; Fig. 1, lanes 1, 3). We set out to isolate, identify, and characterize this protein antigen, Vp67, by using oocytes instead of fertilized eggs as the protein source, owing to the relative ease in obtaining large amounts of starting material. As a first step toward identification of Vp67, we asked whether the protein was conserved among various species. Indeed, we found that the anti-Vp67 monoclonal antibody recognizes proteins from several different organisms, including human (Fig. 1, lane 2) and *Drosophila melanogaster* (lane 4). Moreover, the apparent molecular mass of human protein recognized by anti-Vp67 antibody, is similar to that of *Xenopus* Vp67 (Fig. 1, lanes 1–3). These results suggest that Vp67 protein may be well conserved, particularly among vertebrates.

Subcellular Distribution of Vp67

To determine the subcellular distribution of the Vp67 protein, we fractionated *Xenopus* oocytes and used Western blot analysis with anti-Vp67 antibody to monitor the presence of the Vp67 protein. Crude oocyte homogenates were first centrifuged at 16,000 $\times$ *g*, followed by centrifugation of the supernatant at 100,000 $\times$ *g*. The resulting pellet (P) and supernatant (S) fractions contain crude preparations of membrane and soluble proteins, respectively. As shown in Figure 2 (lanes 1, 2), Vp67 protein is predominantly present in the membrane fraction (P, lane 1). To determine whether Vp67 might be a peripheral or integral membrane protein, we used high salt treatment (as in Thomas and McNamee, 1990). We treated the oocyte membrane pellet (P) with 1 M KCl followed by centrifugation at 100,000 $\times$ *g*. Vp67 was not solubilized by this treatment (Fig. 2, lanes 3, 4) and remained in the pellet fraction (PK, lane 3). These results indicate that Vp67 is either an integral membrane protein or is contained within a membrane-bound organelle.

Purification of Vp67

To extract Vp67 from the membrane fraction for purification, we tested a variety of detergents, including nonionic, zwitterionic, and ionic detergents. Vp67 protein was efficiently extracted from the pellet by anionic detergents such as sodium deoxycholate or sodium cholate (data not shown). Of the nondenaturing detergents tested, only two (MEGA-9 and Empigen BB) were capable of extracting Vp67 from the membrane fraction. Most, however, were not effective in solubilizing Vp67, as shown

for Triton X-100 (Fig. 3A, lanes 2, 3). Notably, although Triton X-100 does not effectively solubilize Vp67 protein (Fig. 3A, lane 3), extraction of other proteins is quite efficient, as monitored by Coomassie Blue protein staining (Fig. 3B, lane 3). Based on these results, a two-step differential detergent extraction strategy was established. The crude membrane fraction (P; Fig. 3A,B, lanes 1) was extracted with Triton X-100 followed by centrifugation to generate supernatant S1 and pellet P1, which is enriched for Vp67 protein (Fig. 3A,B, lanes 2, 3). Next, Vp67 protein was solubilized from pellet P1 by extraction with MEGA-9 (Fig. 3A,B, lanes 4, 5). This strategy yields a soluble fraction, S2 (Fig. 3A,B, lanes 5) that is highly enriched for Vp67.

For the final step in purification of Vp67, immunoaffinity chromatography was used, with anti-Vp67 monoclonal antibodies (Denegre et al., 1997). First, anti-Vp67 antibodies were bound and crosslinked to anti-IgM coated magnetic beads. Next, Vp67-enriched supernatant S2 (Fig. 4, lane 1) was incubated with the anti-Vp67–coated beads. Bound Vp67 was eluted from the beads and resolved by sodium dodecyl sulfate-polyacrylamide gel electrophoresis (SDS-PAGE; Fig. 4, lanes 2, 3). Purified Vp67 protein consists of a doublet, visualized by both Western blot (Fig. 4, lane 2) and protein staining (Fig. 4, lane 3). Both bands appeared to represent the same protein by matrix assisted laser desorption ionization mass spectrometry (MALDI-MS) protein identification analysis. The sequences of two peptides were determined, and both showed high homology to the mitochondrial protein dihydrolipoamide acetyltransferase (Thekkumkara et al., 1988; Matuda et al., 1992), which is the E2 component of the pyruvate dehydrogenas complex (PDC-E2). These results suggest that Vp67 may be *Xenopus* PDC-E2.

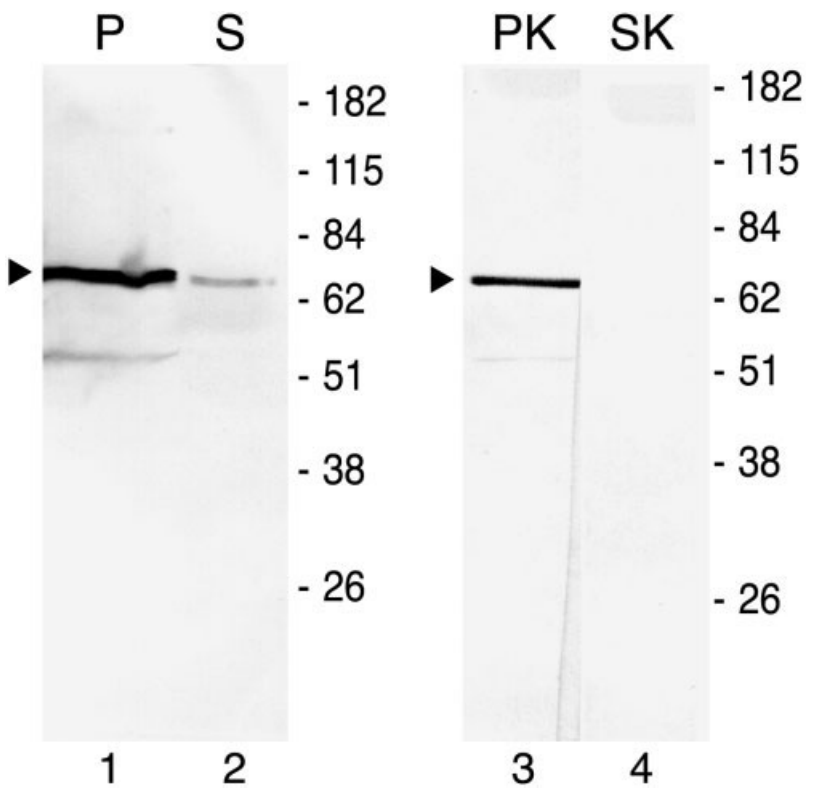

Fig. 2. Subcellular distribution of the Vp67 in *Xenopus* oocytes. Oocyte homogenates were centrifuged at 100,000 × *g* for 2 hr to generate pellet (P, lane 1) and soluble (S, lane 2) fractions. The pellet was extracted with 1 M KCl, followed by centrifugation at 100,000 × *g* for 2 hr, to generate a KCl-insoluble pellet (PK, lane 3) fraction and a KCl-soluble fraction (SK, lane 4). Each fraction contained ~200 μg of total protein, which was separated by 10% sodium dodecyl sulfate-polyacrylamide gel electrophoresis and blotted with anti-Vp67 antibody. Molecular mass markers (in kDa) are noted at the right, and the position of Vp67 is indicated by arrowheads.

Cloning of Vp67 cDNA

The determined peptide sequences obtained from purified *Xenopus* Vp67 were used to design degenerate oligonucleotides for PCR. Additional primers were based on available vertebrate PDC-E2 cDNA sequences (Thekkumkara et al., 1988; Matuda et al., 1992). Two overlapping PCR products (~200 bp and 400 bp) were successfully amplified from *Xenopus* total oocyte cDNA. On the basis of the nondegenerate sequences of the PCR products, we designed primers to obtain overlapping 5′ and 3′ Vp67 cDNA clones by using a rapid amplification of cDNA ends (RACE) strategy (Frohman, 1994). We obtained 3′ RACE products of ~0.6 kb and 5′ RACE products of ~1.7 kb. All 5′ RACE clones contained an ~130-bp 5′ untranslated region (UTR) followed by an open reading frame (ORF) of 1,602 bp. The 3′ RACE clones contained 361 bp of continuous ORF, followed by a stop codon and ~130 bp of 3′ UTR. Sequence compilation of the overlapping 5′ and 3′ RACE cDNA clones reveals a complete ORF of 1,884 bp, encoding a protein of 628 amino acids (Fig. 5A). The cloned cDNA sequences correspond to ~2.1 kb, and, by using Northern blot analysis of poly(A)$^+$ RNA from *Xenopus* oocytes, we detect a transcript of the appropriate size (Fig. 5B).

Vp67 Is a *Xenopus* Homolog of PDC-E2

Sequence and database analyses showed Vp67 to be a *Xenopus* homolog of the mitochondrial protein dihydrolipoamide acetyltransferase (PDC-E2), as predicted from the sequenced peptides. As shown in Figure 5A, *Xenopus* Vp67 is highly related to human PDC-E2 (Thekkumkara et al., 1988), with overall amino acid identity of ~82% for the mature protein. The two peptide sequences obtained from the purified Vp67 are present in the translated cDNA sequence (boxed, Fig. 5A), and the calculated molecular mass of 61 kDa correlates

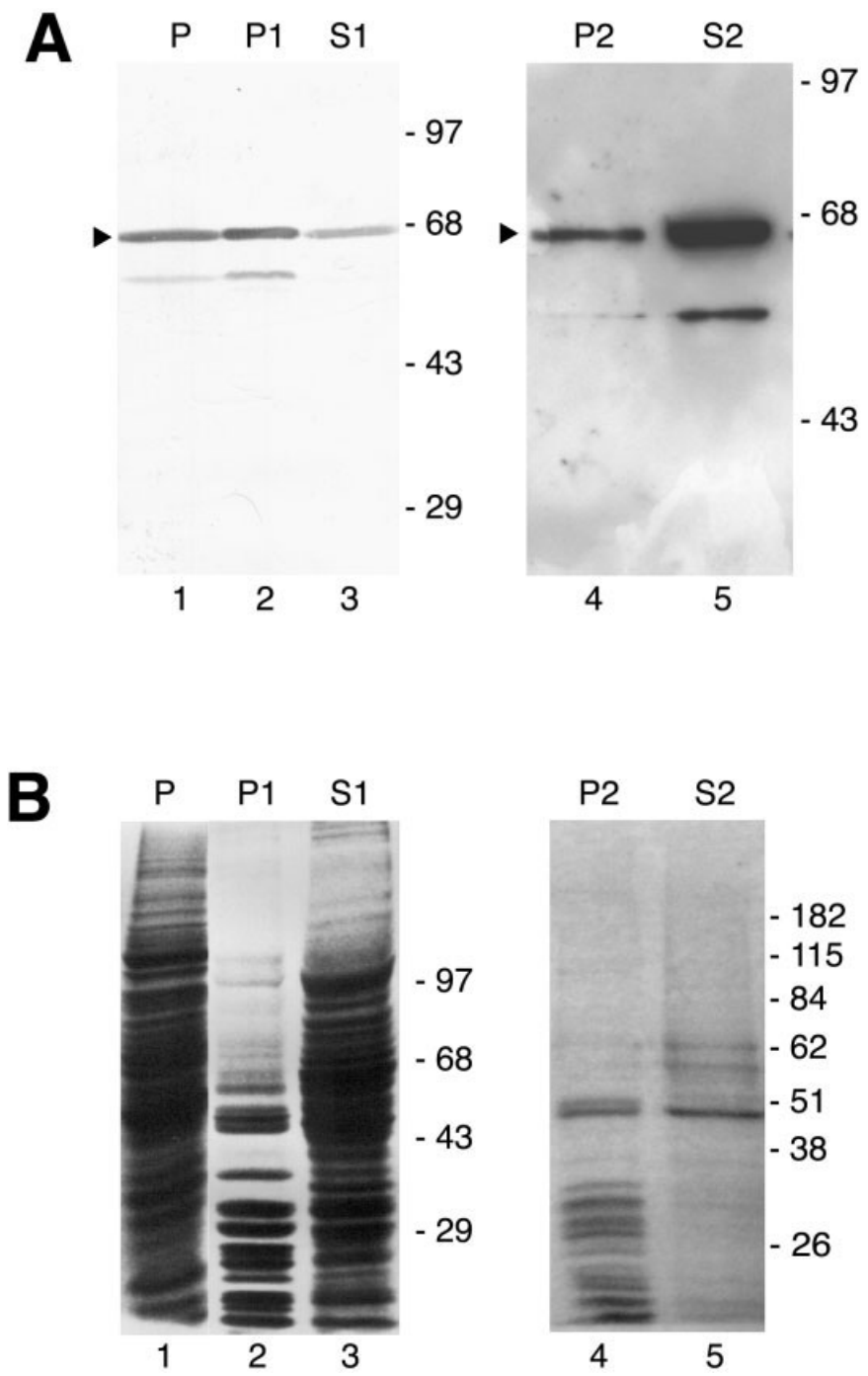

Fig. 3. Two-step differential detergent extraction of Vp67. Oocyte membrane fractions (P, lanes 1) were extracted with 0.2% Triton X-100, followed by centrifugation at 100,000 × *g* for 2 hr to generate pellet P1 (lanes 2) and supernatant S1 (lanes 3) fractions. Pellet P1 was subsequently extracted with 0.5% MEGA-9, resulting in pellet P2 (lanes 4) and supernatant S2 (lanes 5) after centrifugation at 100,000 × *g* for 2 hr. **A:** Protein fractions were separated by 10% sodium dodecyl sulfate-polyacrylamide gel electrophoresis (SDS-PAGE), followed by Western blot analysis by using anti-Vp67 with colorimetric detection (lanes 1–3) or enhanced chemiluminescence detection (lanes 4, 5). The position of Vp67 protein is indicated by arrowheads. **B:** After separation by 10% SDS-PAGE, total protein was visualized by Coomassie Blue protein staining (lanes 1–5). Molecular mass markers are noted (in kDa) at the right of each panel.

well with the apparent molecular mass of ~67 kDa for Vp67 as determined by SDS-PAGE. The ~6 kDa discrepancy is likely explained by post-translational attachment of lipoate residues (Guest et al., 1985), which has been observed to decrease electrophoretic mobility of the protein (Hummel et al., 1988). As shown in Figure 1, anti-Vp67 monoclonal antibodies recognize a human protein of ~67 kDa (Fig. 1, lane 2), and this is the expected mobility of mammalian PDC-E2 (De Marcucci et al., 1988). Moreover, the molecular mass of *Drosophila* protein recognized by anti-Vp67 (~ 54 kDa; Fig. 1, lane 4), is as predicted for the putative *Drosophila* dihydrolipoamide acetyltransferase (Genbank accession no. AAF52514). Taken together, these results indicate that Vp67 is *Xenopus* dihydrolipoamide acetyltransferase (PDC-E2).

The *Xenopus* PDC-E2 cDNA sequence contains all domains characteristic of dihydrolipoamide acetyltransferase (Bleile et al., 1981; Packman et al., 1984; De Marcucci et al., 1988; Thekkumkara et al., 1988; Russell and Guest, 1991; Matuda et al., 1992), including a mitochondrial targeting signal, two lipoyl-binding domains, a conserved E1/E3 subunit binding domain, and a CoA binding site within the conserved C-terminal catalytic domain (Fig. 5A). PDC-E2 is encoded by a nuclear gene and is synthesized as a precursor with an N-terminal leader sequence, which is subsequently cleaved to generate the mature protein in the mitochondria (De Marcucci et al., 1988). A putative mitochondrial leader sequence is present in *Xenopus* PDC-E2 (Claros and Vincens, 1996), with Ser68 encoding the first amino acid of the mature protein (Fig. 5A). The PDC carries out the conversion of pyruvate to acetyl-CoA upon entry into the mitochondria. This oxidative decarboxylation of pyruvate is carried out in a sequential manner by the catalytic components of this multienzyme complex, PDC-E1 (pyruvate dehydrogenase), PDC-E2 (dihydrolipoamide acetyltransferase), and PDC-E3 (dihydrolipoamide dehydrogenase; reviewed in Patel and Roche, 1990; Reed and Hackert, 1990). Decarboxylation of pyruvate

is catalyzed by PDC-E1, which then links the resulting acetyl group to a lipoyl moiety that is covalently bound to PDC-E2. PDC-E2 then carries out transfer of the acetyl group to CoA bound at its active site, generating acetyl-CoA. The PDC-E2–bound lipoyl group is reduced during the initial transfer and is subsequently reoxidized by PDC-E3 in an NAD^+-dependent reaction (Patel and Roche, 1990; Reed and Hackert, 1990). The catalytic domain of PDC-E2 is apparent in the *Xenopus* cDNA sequence (Fig. 5A) and contains the conserved CoA binding site (Russell and Guest, 1991). As also expected, the *Xenopus* PDC-E2 sequence (Fig. 5A) contains two lipoic acid binding domains that are highly homologous to those found in PDC-E2 from other vertebrates (Thekkumkara et al., 1988; Matuda et al., 1992). In addition to its central catalytic role, PDC-E2 is also the structural core of the complex (Stoops et al., 1997) and contains domains that mediate interactions with PDC-E1 and PDC-E3 (Fig. 5A).

As a final test of whether Vp67 protein is indeed a frog homolog of PDC-E2, we next tested whether antibodies specific to human PDC-E2 (hPDC-E2) are capable of recognizing *Xenopus* Vp67. The presence of autoantibodies to mitochondria, especially to the E2 component of pyruvate dehydrogenase complex, is a serologic hallmark of primary biliary cirrhosis (PBC) in human patients (reviewed in Gershwin et al., 2000; Mackay et al., 2000). We used hPDC-E2–specific PBC patient serum (Nishio et al., 1997) to probe frog oocyte proteins by Western blot analysis. As shown in Figure 6A (lane 1), anti–hPDC-E2 recognizes a *Xenopus* antigen of ~67 kDa. Next, we performed immunoprecipitation from *Xenopus* oocyte extracts using anti-Vp67 antibody and analyzed the bound (B) and unbound (U) proteins by Western blot analysis with anti–hPDC-E2 (Fig. 6A) and anti-Vp67 (Fig. 6B) control antibodies. Indeed, the anti–hPDC-E2 recognizes the *Xenopus* protein bound by anti-Vp67 antibodies (Fig. 6A, lane 3), further confirming that Vp67 is *Xenopus* PDC-E2.

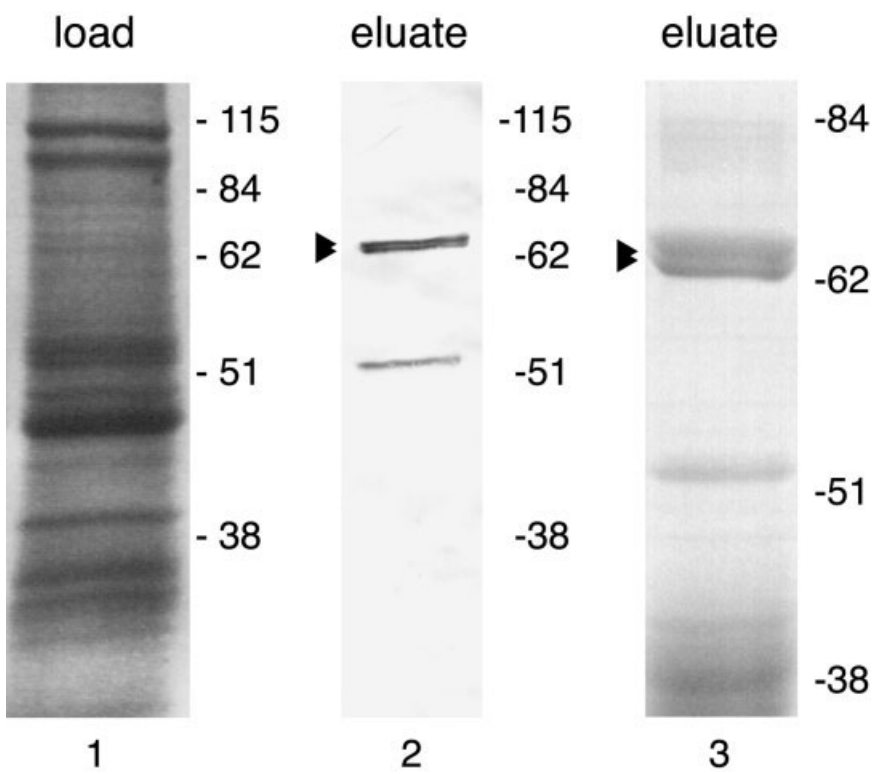

Fig. 4. Immunopurification of Vp67. Vp67-enriched MEGA-9 supernatant S2 (lane 1) was applied to the anti-Vp67–coated magnetic beads for immunopurification. Vp67 was eluted from the beads (lanes 2, 3) by boiling in sample buffer. Load (lane 1) and eluate (lanes 2, 3) fractions were resolved by 10% sodium dodecyl sulfate-polyacrylamide gel electrophoresis followed by Coomassie Blue staining (lanes 1, 2) or Western blotting with anti-Vp67 antibody (lane 3). Molecular mass markers (in kDa) are noted at the right of each panel.

DISCUSSION

Several lines of evidence identify Vp67 as a mitochondrial protein. The sequences of tryptic peptides obtained from purified Vp67 show high similarity to known PDC-E2 protein sequences, the cloned Vp67 cDNA is highly homologous to vertebrate PDC-E2 sequences and antisera specific for PDC-E2 recognize Vp67 protein. The apparent localization of Vp67 to the vegetal hemisphere of *Xenopus* eggs is intriguing and could result from asymmetry of mitochondrial organization and/or localization in *Xenopus* eggs. Notably, a second monoclonal antibody that differentially stains the vegetal cortex of the egg (D4-4G8; Denegre et al., 1997) also recognizes a mitochondrial protein, in this case F_1 ATPase (N. Volodina, J.M. Denegre, and K.L. Mowry, unpublished results). Asymmetric distributions of mitochondria have been observed during oogenesis and early embryonic development in several organisms (Mignotte et al., 1987; Bement and Capco, 1990; Elinson et al., 1993; Calarco, 1995; Yost et al., 1995; Bavister and Squirrell, 2000; Motta et al., 2000). Despite the general uniformity of mitochondria, their size, structure, and/or number may be modified to meet changing requirements (reviewed in Bereiter-Hahn and Voth, 1994; Lloreta-Trull and Serrano, 1998). For example, mitochondria are frequently found as reticular networks, rather than as the classic kidney bean–shaped organelles (Bereiter-Hahn and Voth, 1994; Yaffe, 1999), and mitochondria differing in matrix density, cristae structure, and density have been reported for a variety of cell types (Flickinger, 1968; Matile and Bahr, 1968; Ord and Smith, 1982). Moreover, it has been hypothesized that several different mitochondrial populations can be present within a cell (reviewed in Yaffe, 1999).

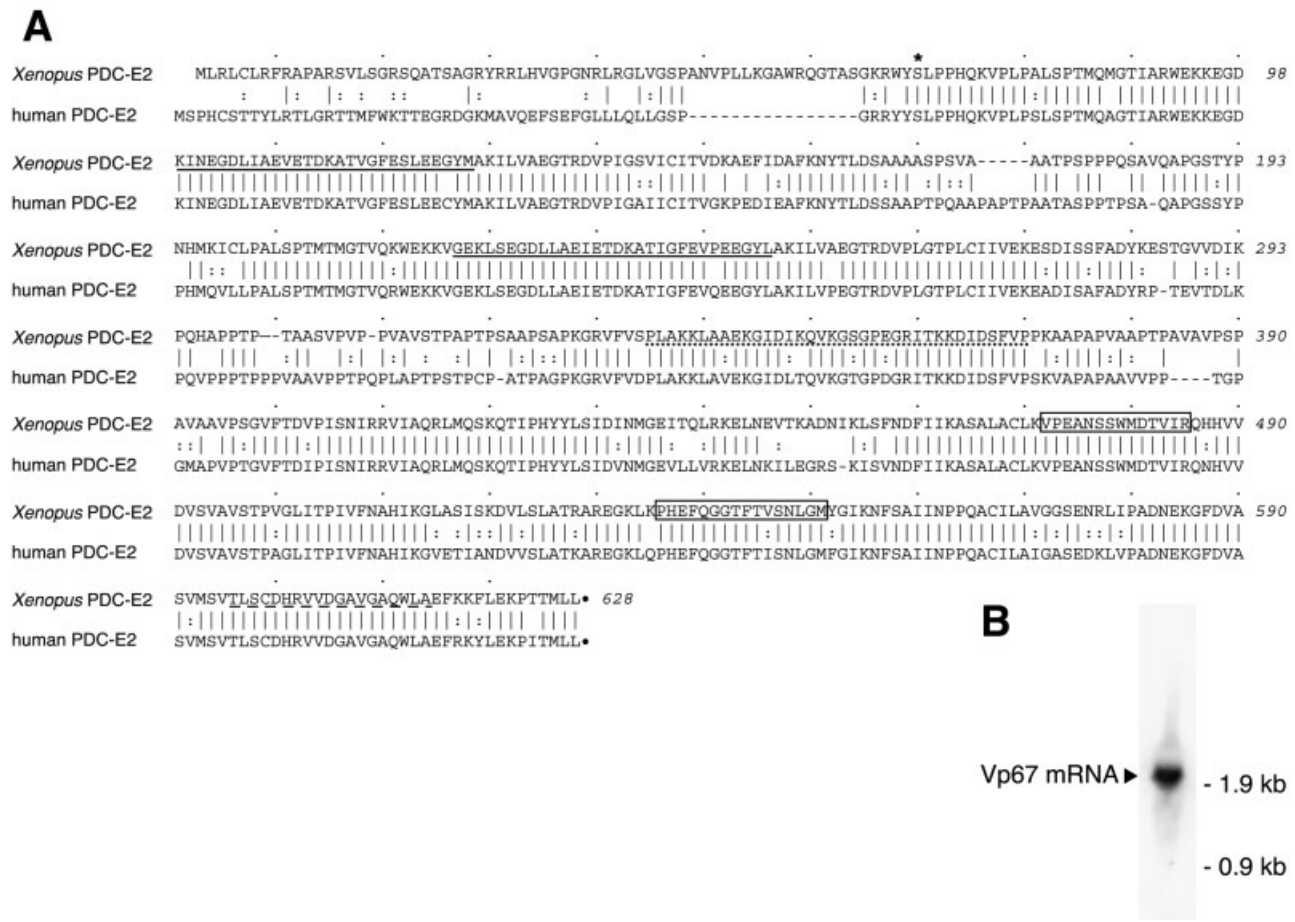

Fig. 5. Cloning of Vp67. **A:** Predicted amino acid sequence of *Xenopus* Vp67 is aligned with the sequence of human PDC-E2 (human dihydrolipoamide S-acetyltransferase, mitochondrial precursor; Genbank accession no. P10515). Identical amino acids are marked by vertical lines, conserved amino acids are marked by vertical double dots, and the positions of the sequenced peptides are boxed. The stop codons are marked by large dots, and the beginning of the mature peptide is marked by an asterisk. Two conserved lipoyl-binding domains are underlined, the E1/E3 binding region is shown by a dotted underline, and the CoA binding site is indicated by a dashed underline. The Genbank accession number for *Xenopus* Vp67 (PDC-E2) is AF4030140. **B:** Northern blot analysis of Vp67 mRNA using poly $(A)^+$ RNA from *Xenopus* oocytes reveals a transcript of ~2.1 kb. The position of Vp67 mRNA is indicated at the left, and size markers (in kb) are noted at the right.

Localization and/or aggregation of mitochondria have been observed during *Xenopus* oogenesis (Heasman et al., 1984; Tourte et al., 1984; Mignotte et al., 1987). During the initial stages of oogenesis, the mitochondrial cloud is a site of active mitochondriogenesis and mitochondrial replication (Heasman et al., 1984). After fragmentation of the mitochondrial cloud in *Xenopus* oocytes, two segregating populations of mitochondria are discernible (Tourte et al., 1984; Mignotte et al., 1987). One population remains around the nucleus, actively replicating mitochondrial DNA (mtDNA) and ultimately generates the majority of the mitochondria in the fully grown oocyte (Tourte et al., 1984; Mignotte et al., 1987). The other population moves toward the vegetal cortex and stops replicating mtDNA early in vitellogenesis (Mignotte et al., 1987). Organelles of this population are considered to be the components of the germ plasm (Heasman et al., 1984; Mignotte et al., 1987), which is a defined localization of maternal cytoplasmic components that are thought to determine the germline (reviewed in Wylie, 1999). Clusters of mitochondria are known to be associated with *Xenopus* germ plasm material (Williams and Smith, 1971; Heasman et al., 1984; Savage and Danilchik, 1993); however, the functional significance of this association remains unclear. The apparent localization of Vp67 (*Xenopus* PDC-E2) may be related to the restriction of germ plasm to the vegetal cortex. Additionally, our results may further reflect an underlying asymmetry in mitochondrial organization and/or localization during early development, which will warrant further investigation.

EXPERIMENTAL PROCEDURES

Oocytes, Embryos, and Cells

Oocytes were obtained surgically from adult female *Xenopus laevis* frogs (*Xenopus* I) and defolliculated by treatment with 0.2% collagenase (Sigma, type I) in $OR2^-$ buffer (82 mM NaCl, 2.5 mM KCl, 1.5 mM Na_2HPO_4, 50 mM HEPES pH 7.6). *Drosophila*

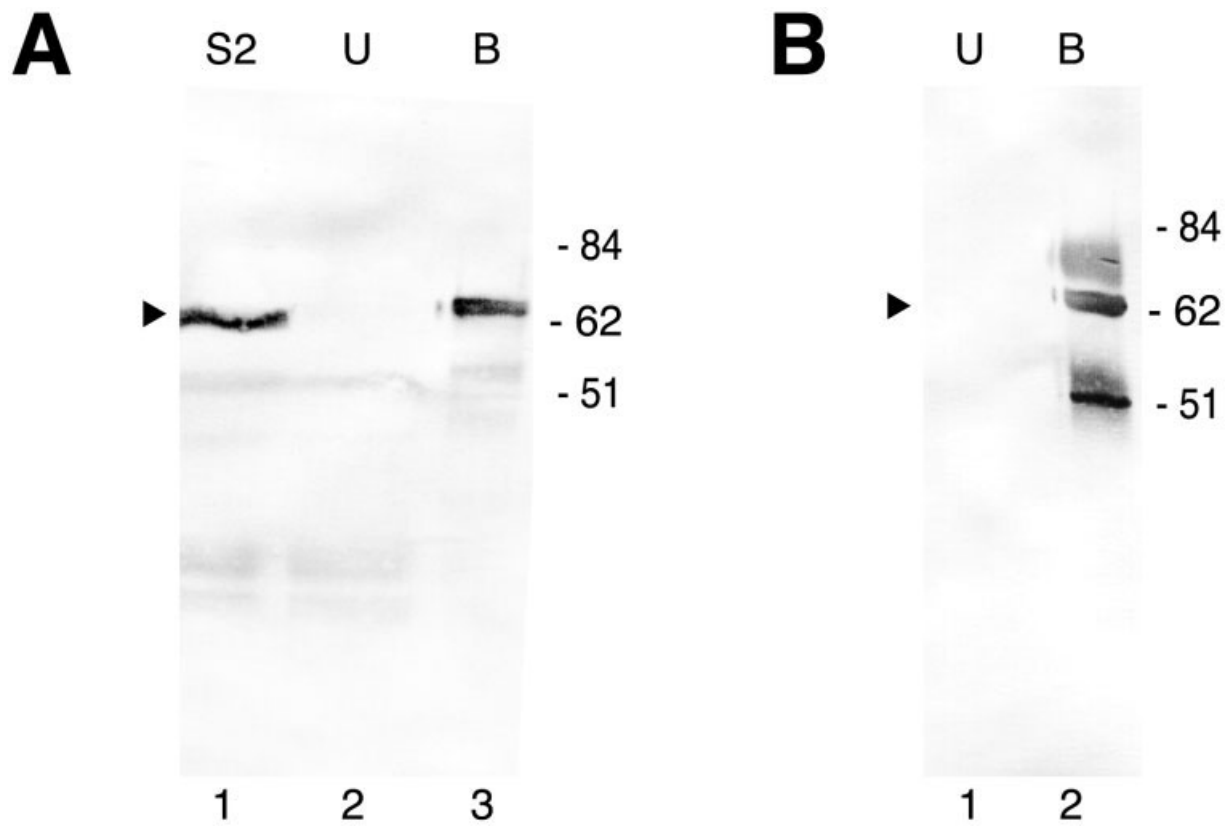

Fig. 6. Vp67 protein is the E2 component of the pyruvate dehydrogenase complex (PDC-E2). *Xenopus* oocyte homogenates were fractionated as in Figure 3, and Vp67-enriched fraction S2 (lane 1 in A) was applied to anti-Vp67–coated beads. Bound (*Xenopus* Vp67, lane 3 in A and lane 2 in B) and unbound (lane 2 in A and lane 1 in B) fractions were separated by 10% sodium dodecyl sulfate-polyacrylamide gel electrophoresis. **A:** Western blot analysis was performed with human anti–hPDC-E2 antibodies, which recognize *Xenopus* Vp67. **B:** Western blot analysis was performed with anti-Vp67 monoclonal antibody. Anti-Vp67 was not crosslinked to the beads, and eluted antibody molecules are apparent in the Western blot of the eluted fraction (lane 1). Molecular weight markers in kDa are noted at the right, for each panel.

melanogaster early cleavage embryos were kindly provided by Dr. K. Wharton (Brown University). Human leukemia cells (HL-60) were kindly provided by Dr. Z. Han (Brown University).

Antibodies

Anti-Vp67 monoclonal antibody (MAb) has been described previously (D5-5G7; in Denegre et al., 1997). Hybridoma cell cultures were grown in Iscove's modified Dulbecco's modified Eagle medium supplemented with 15% fetal calf serum, 50 mg/ml gentamicin and 2 mM glutamine (Gibco BRL). Tissue culture supernatant was collected and stored at −20°C until use. Antibody class isotyping was performed by using Isostrip Mouse Monoclonal Antibody Isotyping Kit (Boehringer/Roche). Human autoimmune antisera against human PDC-E2 from primary biliary cirrhosis (PBC) patients (Nishio et al., 1997) was kindly provided by Dr. M.E. Gershwin and Dr. P.S. Leung (UC Davis, School of Medicine).

Western Blotting

Protein samples were separated by SDS-PAGE and transferred to nitrocellulose. Gels run in parallel were stained with Coomassie Blue (Sigma) to visualize total protein. The filters were washed in blotto (50 mM Tris pH 7.5, 185 mM NaCl, 0.05% Tween 20, 3% w/v nonfat dry milk) and incubated 2 hr at room temperature with anti-Vp67 MAb (diluted 1:1 in blotto). After washing for 1 hr in blotto, peroxidase- or alkaline phosphatase-conjugated goat anti-mouse IgM antibody (Sigma or Jackson ImmunoResearch Laboratories) was used as a secondary antibody. Filters were washed for 30 min in blotto without milk, and detection was performed by enhanced chemiluminescence or by colorimetric detection (Boehringer/Roche).

Oocyte Fractionation

Defolliculated oocytes were washed three times with $OR2^-$ and homogenized in equal volume of S100 buffer (50 mM Tris pH 9, 50 mM KCl, 0.1 mM ethylenediaminetetraacetic acid, 25% glycerol, 1 mM dithiothreitol). After centrifugation at 16,000 × *g* for 15 min at 4°C, the supernatant (oocyte homogenate) was centrifuged for 2 hr at 100,000 × *g* at 4°C. The soluble (S, supernatant) and membrane (P, pellet) fractions were aliquoted and held at −80°C until use. Total protein concentration was determined by using Bradford-based Protein Assay (Bio-Rad). For KCl-extraction, oocyte membrane fraction (P) at final protein concen-

tration of 1–2 mg/ml was incubated with 1 M KCl for 1 hr at 4°C followed by centrifugation for 2 hr at 100,000 × *g* to generate supernatant (SK) and pellet (PK) fractions. For two-step detergent extraction, the oocyte membrane fraction (P) was incubated for 10–15 min at 4°C with 0.2% Triton X-100 (Sigma) in S100 buffer, followed by centrifugation at 100,000 × *g* for 2 hr. The supernatant (S1) was removed, and the pellet (P1) was immediately incubated in 0.5% MEGA-9 (Calbiochem) in 150 mM NaCl, 10 mM Tris, pH 8, and protease inhibitors (1 mM Pefabloc (Roche) and 1 μg/ml each leupeptin, antipain, and trypsin inhibitor (Sigma)), with gentle mixing for 18–20 hr at 4°C. After centrifugation for 1 hr at 100,000 × *g*, the resulting supernatant (S2), containing solubilized Vp67 protein, was used for immunoaffinity purification.

Immunoaffinity Purification

Anti-IgM–coated paramagnetic beads (Dynal) were incubated with constant mixing for 2 hr at 4°C with anti-Vp67 MAb. After washing three times with PBS/0.1% ovalbumin, anti-Vp67 was crosslinked to the beads using DMP (Sigma), according to the protocol supplied by the manufacturer (Dynal), with ovalbumin as a blocking agent. The anti-Vp67–coated beads were incubated with the MEGA-9 supernatant (S2, ~10^7 beads/mg S2) for 1 hr at 4°C with constant mixing, followed by three washes with PBS. Bound Vp67 was eluted by boiling in SDS sample buffer, resolved by SDS-PAGE, and cut from the gel. For large-scale purification, ~200 mg of crude oocyte membrane protein fraction (P) was used to obtain ~2 μg of purified Vp67. MALDI-MS analysis and the determination of tryptic peptide sequences was performed by the Keck Foundation Biotechnology Resource Laboratory (Yale University).

Cloning and Analysis of Vp67 cDNA

cDNA was prepared from the oocyte total RNA by using Advantage RT-for-PCR kit (Clontech). Oligonucleotides (AGTCIAARCARACIATWCCICAUTAYTAY, TGRTTUTGIGKWATRACIGTRTCCATCC, and GCIGARAAATKUTTRATICCRWACAT) based on the determined peptide sequences and conserved PDC-E2 sequences (Thekkumkara et al., 1988; Matuda et al., 1992) were used for PCR amplification. The resulting nondegenerate sequence was used to design gene-specific primers (TGCCCACATCAAGGGGCTGGCATCCATCAG and AAGCTTGCCTTCTCGTGCCCGGGTTGCTAG), and full-length cDNA was obtained by using PCR-based RACE cDNA amplification (GeneRacer, Invitrogen). The products were subcloned for sequencing into T7/T3 primer-containing vector by using TOPO TA Cloning Kit (Invitrogen). Sequence analysis and alignments were performed by using the Basic Local Alignment Search Tool (BLAST), ClustalW tools (www.ch.embnet.org), MacVector (Accelrys), and Genetics Computer Group (Madison, Wisconsin) software. Database searches were performed by using SWISS-PROT, PROSITE, and NCBI protein and cDNA databases and searched by using ExPASy search tools. The mitochondrial leader sequence was predicted by using MitoProt II 1.0a4 software application (Claros and Vincens, 1996).

ACKNOWLEDGMENTS

We thank Drs. M.E. Gershwin and P.S. Leung for human PBC autoimmune sera. We also thank Dr. Jim Clifton, Dr. Douglas Hixson, Dr. Jörg Martin, Dr. Gary Wessel, Dr. Joanne Yeh, and the members of Martin and Wessel Labs for experimental advice and use of equipment and Tracy Kress, Ray Lewis, Tim Messitt, and Young Yoon for helpful discussions and for critical reading of the manuscript. This work was funded by a grant to K.L.M. from the NSF.

REFERENCES

Bavister BD, Squirrell JM. 2000. Mitochondrial distribution and function in oocytes and early embryos. Hum Reprod 15(Suppl 2):189–198.

Bement WM, Capco DG. 1990. Transformation of the amphibian oocyte into the egg: structural and biochemical events. J. Electron Microsc Tech 16:202–234.

Bereiter-Hahn J, Voth M. 1994. Dynamics of mitochondria in living cells: shape changes, dislocations, fusion, and fission of mitochondria. Microsc Res Tech 27:198–219.

Bleile DM, Hackert ML, Pettit FH, Reed LJ. 1981. Subunit structure of dihydrolipoyl transferase component of pyruvate dehydrogenase complex from bovine heart. J Biol Chem 256:514–519.

Calarco PG. 1995. Polarization of mitochondria in the unfertilized mouse oocyte. Dev Genet 16:36–43.

Chan AP, Etkin LD. 2001. Patterning and lineage specification in the amphibian embryo. Curr Top Dev Biol 51:1–67.

Chang P, Perez-Mongiovi D, Houliston E. 1999. Organization of *Xenopus* oocyte and egg cortices. Microsc Res Tech 44: 415–429.

Claros MG, Vincens P. 1996. Computational method to predict mitochondrially imported proteins and their targeting sequences. Eur J Biochem 241:779–786.

Danilchik MV, Gerhart J. 1987. Differentiation of the animal-vegetal axis in *Xenopus laevis* oocytes. I. Polarized translocation of platelets establishes the yolk gradient. Dev Biol 122:101–112.

De Marcucci OG, Gibb GM, Dick J, Lindsay JG. 1988. Biosynthesis, import and processing of precursor polypeptides of mammalian mitochondrial pyruvate dehydrogenase complex. Biochem J 251:817–823.

Denegre JM, Ludwig ER, Mowry KL. 1997. Localized maternal proteins in *Xenopus* revealed by subtractive immunization. Dev Biol 192:446–454.

Dumont JN. 1972. Oogenesis in *Xenopus laevis* (Daudin). I. Stages of oocyte development in laboratory maintained animals. J Morphol 136:153–179.

Elinson RP, King ML, Forristall C. 1993. Isolated vegetal cortex from *Xenopus* oocytes selectively retains localized mRNAs. Dev Biol 160:554–562.

Flickinger CJ. 1968. Mitochondrial polymorphism in *Amoeba proteus*. Protoplasma 66:139–150.

Frohman MA. 1994. On beyond classic RACE (rapid amplification of cDNA ends). PCR Methods Appl 4:S40–S58.

Gard D. 1995. Axis formation during amphibian oogenesis: reevaluating the role of the cytoskeleton. Curr Top Dev Biol 30:215–252.

Gard DL. 1999. Confocal microscopy and 3-D reconstruction of the cytoskeleton of *Xenopus* oocytes. Microsc Res Tech 44:388–414.

Gershwin ME, Ansari AA, Mackay IR, Nakanuma Y, Nishio A, Rowley MJ, Coppel RL. 2000. Primary biliary cirrhosis: an orchestrated immune response against epithelial cells. Immunol Rev 174:210–225.

Guest JR, Lewis HM, Graham LD, Packman LC, Perham RN. 1985. Genetic reconstruction and functional analysis of the repeating lipoyl domains in the pyruvate dehydrogenase multienzyme complex of *Escherichia coli*. J Mol Biol 185:743–754.

Heasman J, Quarmby J, Wylie CC. 1984. The mitochondrial cloud of *Xenopus* oocytes: the source of germinal granule material. Dev Biol 105:458–469.

Hummel KB, Litwer S, Bradford AP, Aitken A, Danner DJ, Yeaman SJ. 1988. Nucleotide sequence of a cDNA for branched chain acyltransferase with analysis of the deduced protein structure. J Biol Chem 263:6165–6168.

Lloreta-Trull J, Serrano S. 1998. Biology and pathology of the mitochondrion. Ultrastruct Pathol 22:357–367.

Mackay IR, Whittingham S, Fida S, Myers M, Ikuno N, Gershwin ME, Rowley MJ. 2000. The peculiar autoimmunity of primary biliary cirrhosis. Immunol Rev 174: 226–237.

Matile P, Bahr GF. 1968. Biochemical and quantitative electron microscopic evidence for heterogeneity of mitochondria from *Saccharomyces cerevisiae*. Exp Cell Res 52:301–307.

Matuda S, Nakano K, Ohta S, Shimura M, Yamanaka T, Nakagawa S, Titani K, Miyata T. 1992. Molecular cloning of dihydrolipoamide acetyltransferase of the rat pyruvate dehydrogenase complex: sequence comparison and evolutionary relationship to other dihydrolipoamide acyltransferases. Biochim Biophys 1131:114–118.

Mignotte F, Tourte M, Mounolou JC. 1987. Segregation of mitochondria in the cytoplasm of *Xenopus* vitellogenic oocytes. Biol Cell 60:97–102.

Motta PM, Nottola SA, Makabe S, Heyn R. 2000. Mitochondrial morphology in human fetal and adult female germ cells. Hum Reprod 15(Suppl 2):129–147.

Mowry KL, Cote CA. 1999. RNA sorting in *Xenopus* oocytes and embryos. FASEB J 13:435–445.

Nishio A, Van de Water J, Leung PS, Joplin R, Neuberger JM, Lake J, Bjorkland A, Totterman TH, Peters M, Worman HJ, Ansari AA, Coppel RL, Gershwin ME. 1997. Comparative studies of antimitochondrial autoantibodies in sera and bile in primary biliary cirrhosis. Hepatology 25:1085–1089.

Ord MJ, Smith RA. 1982. Correlation of mitochondrial form and function in vivo: microinjection of substrate and nucleotides. Cell Tissue Res 227:129–137.

Packman LC, Hale G, Perham RN. 1984. Repeating functional domains in the pyruvate dehydrogenase multienzyme complex of *Escherichia coli*. EMBO J 3:1315–1319.

Patel MS, Roche TE. 1990. Molecular biology and biochemistry of pyruvate dehydrogenase complexes. FASEB J 4:3224–3233.

Reed LJ, Hackert ML. 1990. Structure-function relationships in dihydrolipoamide acyltransferases. J Biol Chem 265: 8971–8974.

Russell GC, Guest JR. 1991. Sequence similarities within the family of dihydrolipoamide acyltransferases and discovery of a previously unidentified fungal enzyme. Biochim Biophys Acta 1076: 225–232.

Savage RM, Danilchik MV. 1993. Dynamics of germ plasm localization and its inhibition by ultraviolet irradiation in early cleavage *Xenopus* embryos. Dev Biol 157:371–382.

Stoops JK, Cheng RH, Yasdi MA, Maeng CH, Schroeter JP, Klueppelberg U, Kolodziej SJ, Baker TS, Reed LJ. 1997. On the unique structural organization of the *Saccharomyces cerevisiae* pyruvate dehydrogenase complex. J Biol Chem 272:5757–5764.

Thekkumkara TJ, Ho L, Wexler ID, Pons G, Liu TC, Patel MS. 1988. Nucleotide sequence of a cDNA for the dihydrolipoamide acetyltransferase component of human pyruvate deydrogenase complex. FEBS Lett 240:45–48.

Thomas TC, McNamee MG. 1990. Purification of membrane proteins. Methods Enzymol 182:499–520.

Tourte M, Mignotte F, Mounolou JC. 1984. Heterogeneous distribution and replication activity of mitochondria in *Xenopus laevis* oocytes. Eur J Cell Biol 34: 171–178.

Williams MA, Smith LD. 1971. Ultrastructure of the "germinal plasm" during maturation and early cleavage of *Rana pipiens*. Dev Biol 25:568–580.

Wylie C. 1999. Germ cells. Cell 96:165–174.

Yaffe MP. 1999. The machinery of mitochondrial inheritance and behavior. Science 283:1493–1497.

Yost HJ, Phillips CR, Boore JL, Bertman J, Whalon B, Danilchik MV. 1995. Relocation of mitochondria to the prospective dorsal marginal zone during Xenopus embryogenesis. Dev Biol 170:83–90.